

Velocity-Selective Magnetic-Resonance Laser Cooling

S-Q. Shang, B. Sheehy, P. van der Straten, and H. Metcalf

Physics Department, State University of New York, Stony Brook, New York 11794

(Received 28 March 1990)

We describe a new sub-Doppler cooling scheme that cools atoms to nonzero velocity v_r . The atomic motion in a combined optical standing wave and constant magnetic field induces a velocity-selective magnetic resonance that produces strong cooling for negative laser detuning to $v_r = \omega_Z/2k$, with ω_Z the Larmor frequency. In a one-dimensional optical molasses transverse to a thermal Rb beam we observe the bunching of the atoms into two peaks corresponding to $\pm v_r$. We present a quantitative comparison between our theory and experiment and suggest some applications.

PACS numbers: 32.80.Pj, 42.50.Vk

Recent experiments in laser cooling¹⁻⁴ have resulted in final temperatures well below the Doppler limit $T_D \equiv \hbar\gamma/2k_B$ derived for two-level atoms (γ is the excited-state decay rate). Optical pumping among the ground-state (gs) magnetic sublevels of multilevel atoms has been shown to be responsible for these sub-Doppler temperatures.^{5,6} We report here a totally new cooling phenomenon caused by Zeeman coherences among the ground states. In the models discussed in Refs. 5 and 6, such coherences were induced only by atomic motion and were assumed to be small. In magnetically induced laser cooling⁴ (MILC) the Larmor precession frequency was small compared to the optical pumping rate at the antinodes of the laser field so the Zeeman coherences were strongly damped. Here we describe a new cooling process that achieves sub-Doppler temperatures and is mediated by gs Zeeman coherences.

For two-level atoms, optical coherences between excited and ground states produce Dopplerons^{7,8} and lead to narrow structures in the velocity dependence of the force at high light intensity. They also produce a sign reversal of the damping for small velocity so that atoms are cooled for blue detuning.^{9,10} One interesting effect of Doppleron resonances is that, for red laser detuning, atoms are "cooled" to $|\mathbf{v}| \neq 0$ at high intensity but to $v = 0$ at low intensity. The sign reversal at small velocity has been verified experimentally,¹¹ and cooling to a finite velocity has recently been detected.^{12,13}

In this Letter we explore both theoretically and experimentally the region of MILC, where the Larmor frequency ω_Z is much larger than the optical pumping rate γ_P . In this case gs coherences play an important role in the cooling process. The motion of the atoms in a standing wave results in modulation of the light intensity that induces a magnetic resonance¹⁴ at a particular velocity $v_r = \omega_Z/2k$, where $\omega_Z = g_F\mu_B B/\hbar$ is the Larmor frequency.¹⁵ In fact, this is a stimulated Raman transition between the two ground states that is resonant at $v = v_r$. As a consequence of this velocity-selective resonance the atoms are cooled to nonzero velocity $\pm v_r$ with a velocity spread below the one-dimensional (1D) Doppler limit $v_D = (7k_B T_D/10M)^{1/2} = 10$ cm/s for Rb. In 1D atomic-beam collimation, cooling to $\pm v_r$ causes vanishing of the central peak of the spatial distribution and the ap-

pearance of two symmetrically placed side peaks.

This new cooling process is appropriately described by a quantization axis along the magnetic field, in contrast to Ref. 4, since ω_Z is much larger than the light shifts. For a 1D standing wave of circularly polarized light directed along the z axis in a magnetic field $\mathbf{B} = B\hat{\mathbf{x}}$, the light induces both σ and π transitions.

In order to gain some physical insight, we study a model $J = \frac{1}{2} \rightarrow \frac{3}{2}$ optical transition whose gs magnetic sublevels are denoted by $|1\rangle$ ($|2\rangle$) for $M_J = -\frac{1}{2}$ ($\frac{1}{2}$) for low excitation rate so we can adiabatically eliminate the excited states.⁴ Then the optical Bloch equations¹⁶ (OBE's) for the gs density matrix ρ become

$$\frac{d\boldsymbol{\sigma}}{dt} = \begin{pmatrix} -\gamma_P & \omega_Z & 0 \\ -\omega_Z & -\gamma'_P & \tilde{\omega}_{12} \\ 0 & -\tilde{\omega}_{12} & -\gamma'_P \end{pmatrix} \boldsymbol{\sigma} + \begin{pmatrix} \gamma_P \\ 0 \\ 0 \end{pmatrix}, \quad (1)$$

where $\boldsymbol{\sigma}$ is the Bloch vector whose components are $\sigma_1 = \rho_{12} + \rho_{21}$, $\sigma_2 = -i(\rho_{12} - \rho_{21})$, and $\sigma_3 = \rho_{22} - \rho_{11}$. The coefficients in Eq. (1) can be readily obtained by transformation from the basis chosen in Ref. 4. We find that $\gamma_P = 4\gamma_S \cos^2(kz)/9L$ and $\gamma'_P = \frac{3}{2}\gamma_P$ are the optical pumping rate and dephasing rate, respectively,¹⁷ and $\hbar\tilde{\omega}_{12} = -4\hbar\delta_S \cos^2(kz)/3L$ is the difference of the light shifts of the two ground states as defined in the basis of Ref. 4 with $\delta = \text{detuning} = \omega_{\text{laser}} - \omega_{\text{atom}}$, $L = 1 + (2\delta/\gamma)^2$, $s = \text{saturation parameter} = 2\Omega_0^2/\gamma^2$, and Ω_0 the Rabi frequency for one beam.

An approximate solution for the OBE's can be found analytically by making a transformation of the Bloch vector to a frame rotating with a frequency $2kv$ and eliminating the fast-oscillating terms with frequencies $\pm 2kv$ and $\pm 4kv$. This rotating-frame approximation requires $|\omega_Z - 2kv| \ll \omega_Z$ and $\tilde{\omega}_{12} \ll \omega_Z$. The optical force¹⁸ exerted on the atoms is obtained from $\mathbf{F} = -\text{Tr}(\rho\nabla H)$ averaged over a wavelength. We find

$$F = \frac{\beta(v - v_r)}{1 + [(v - v_r)/v_c]^2} \quad (2)$$

with the damping constant β and the capture range v_c given by

$$\beta = \hbar k^2 \frac{24\delta\gamma}{25\gamma^2 + 30\delta^2}, \quad (3a)$$

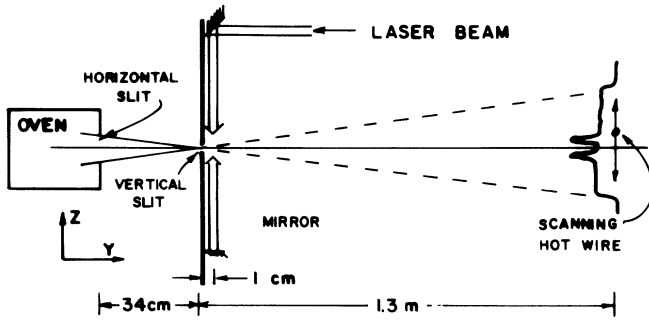


FIG. 1. Schematic diagram of apparatus.

and

$$v_c = \frac{\bar{\gamma}_P}{k} \left(\frac{25\gamma^2 + 30\delta^2}{256\gamma^2} \right)^{1/2}, \quad (3b)$$

where $\bar{\gamma}_P = \gamma_P(z=0)$. This is a cooling force when $\delta < 0$. We note that β is independent of s , and both β and v_c are of the same order of magnitude as those calculated as for other sub-Doppler cooling schemes.⁴⁻⁶ We emphasize that the atoms will not be cooled to $v=0$ as in the other cooling schemes, but to $v_r \neq 0$.

We can learn about the qualitative behavior of the Bloch vector σ that satisfies Eq. (1) by analogy to magnetic resonance. These OBE's are very similar to those describing the evolution of two states separated by ω_Z , driven by a field that induces transitions at a rate $\tilde{\omega}_{12}$. This field oscillates at frequency $2kv$ because a moving atom experiences modulation of the light shift at this frequency due to the periodicity $\lambda/2$ of the standing wave.¹⁴

At resonance ($2kv = \omega_Z$), σ_1 oscillates in phase with $\tilde{\omega}_{12}$ and the force $F = \hbar \nabla \tilde{\omega}_{12} \sigma_1 / 2$ vanishes. At slightly higher or lower velocity σ_1 will be slightly out of phase and the resulting force will cool the atoms to the resonance velocity if $\delta < 0$.

We have demonstrated the cooling of atoms to $v = \pm v_r$ in a 1D collimation experiment in Rb. We used the apparatus of Ref. 4 with the following minor changes (Fig. 1). The collimating aperture is now a vertical slit that provides good horizontal localization of the atoms, and the oven aperture is a horizontal slit that provides a wide range of transverse velocities without rapid consumption of its load of Rb. Each slit is $100 \mu\text{m}$ wide and $\sim 3 \text{ mm}$ long, and the scanning hot-wire detector measures the unperturbed atomic-beam profile to be uniformly flat across its $\sim 12 \text{ mm}$ width. The light from an injection-locked diode-laser array¹⁹ is frequency locked by splitting off part of the light from the master laser, shifting its frequency with an acousto-optic modulator, and locking to a saturated absorption signal from a Rb vapor cell at room temperature. A 1D optical molasses is formed by reflecting the circularly polarized light, and the magnetic field is applied perpendicular to the \mathbf{k} vectors of the laser beams.

We have observed double peaks of width much less than v_D whose separation increases with B over a wide range of parameters. Figure 2 shows a sample of these data for detuning $\delta \sim \pm 0.67\gamma$ taken at the low intensity $s=0.3$. At small field we observe a cold peak⁴ at $v=0$, but at larger fields we see the splitting into two peaks for

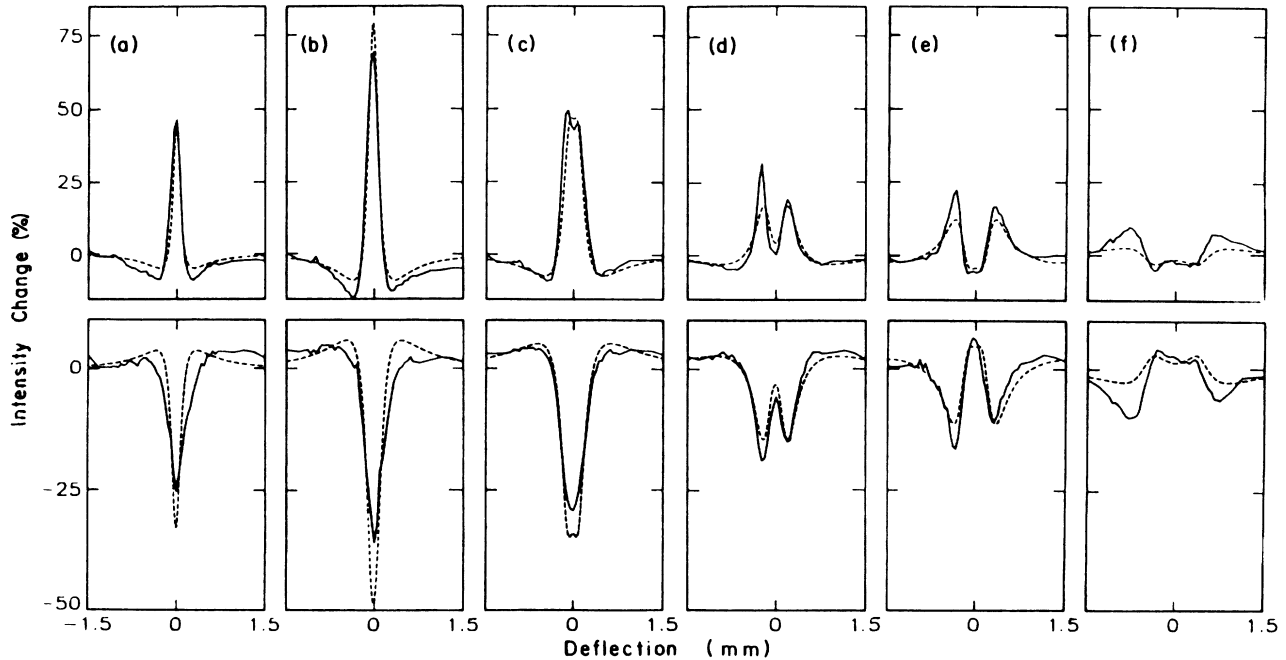


FIG. 2. The change in atomic-beam profile of ^{85}Rb 1.3 m downstream from the molasses as measured by the hot wire for red (top) and blue (bottom) detuning. The laser parameters are $s=0.25$ and $\delta = \pm 0.67\gamma$ and the magnetic field is (a) 0.057 G, (b) 0.114 G, (c) 0.23 G, (d) 0.40 G, (e) 0.57 G, and (f) 1.14 G. The solid lines are experimental data and the dashed lines are the results from the model.

$\delta < 0$, and cooling to a single narrow peak for $\delta > 0$. We emphasize that cooling to $v=0$ with $\delta > 0$ here is different from Ref. 11 because it involves gs Zeeman coherences instead of optical coherences between excited and ground states so it works even at low intensity.

A direct measurement without any deconvolution shows a width of 2.5 cm/s for the peaks of Fig. 2(d), well below $v_D=10$ cm/s. At high magnetic field the peaks are broader since we measure the spatial distribution and atoms with transverse velocity $=v_r$ spread out differently due to the thermal distribution of their longitudinal velocities. Since the relaxation time of the atoms is determined by the optical pumping rate γ_P , we would expect a temperature on the order of $\hbar \gamma_P/k_B$ that could become arbitrarily small since γ_P is proportional to intensity.⁵ However, a lower limit arises when the velocity capture range of the cooling force becomes comparable to the velocity spread,⁵ and from Eqs. (3) we find that this occurs near $s=0.1$.

Figure 3 shows the separation between the peaks versus B for $\delta < 0$ for a variety of detunings and intensities for the $F=3 \rightarrow 4$ transition of ^{85}Rb and the $F=2 \rightarrow 3$ transition of ^{87}Rb . The solid lines represent the resonance condition $2kv = \omega_Z$ with the appropriate g_F factor for ω_Z . The data satisfy this condition except at small magnetic field where it no longer holds because $\omega_Z \gg \bar{\omega}_{12}$ is no longer satisfied.

In order to explain why the resonance condition obtained from the $J = \frac{1}{2} \rightarrow \frac{3}{2}$ model applies equally well for the more complicated ^{85}Rb and ^{87}Rb , we calculate the relative strength of all the allowed pairs of optical transitions connecting ground states. Those connecting

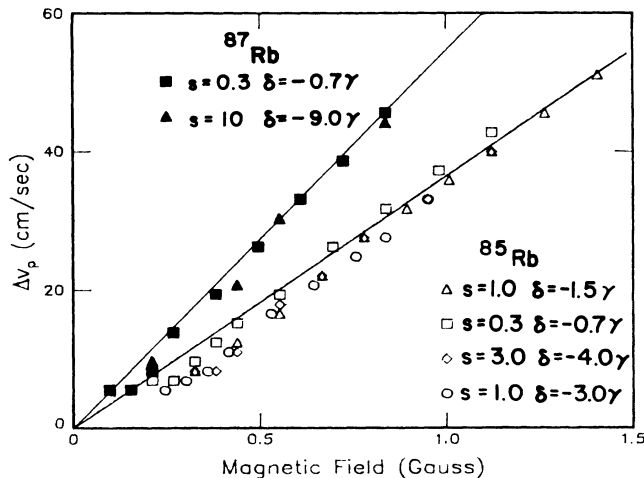


FIG. 3. The separation between the peaks for many data sets, including those of Fig. 2, vs magnetic-field strength for the $F=3 \rightarrow 4$ transition in ^{85}Rb and the $F=2 \rightarrow 3$ transition in ^{87}Rb . Symbols denote experimental points for various intensities ($0.25 \leq s \leq 10$) and detunings ($1 \leq |\delta| \leq 10\gamma$), where we used the average longitudinal velocity ($v \sim 350$ m/s) to convert the deflection angle into a transverse velocity. The solid lines are for the resonance condition.

gs pairs whose M_F values differ by 1 are much more numerous and stronger than those whose M_F values differ by 2, and higher differences are forbidden. Thus the strongest resonance of the real Rb atom is the same as for the simple model, and the other allowed one at $2kv = 2\omega_Z$ is much weaker.

We have extended the $J = \frac{1}{2} \rightarrow \frac{3}{2}$ model to the $F=3 \rightarrow 4$ transition in ^{85}Rb , made a Fourier expansion of the components of σ , and numerically evaluated the coefficients as in Ref. 4. Then we calculate the force versus velocity as shown in Fig. 4 for several values of B , s , and δ corresponding to our experiments.

At small B we see a force damping atoms to $v=0$ as in Ref. 4, but this damping decreases at stronger fields because the efficiency of the optical pumping process is decreased by the field. When the field is strong enough for the splitting between the ground states ω_Z to exceed their widths $\bar{\gamma}_P$ so that they are resolvable, a strong resonance appears around $2kv = \omega_Z$. At higher pumping rate there are also higher-order resonances. These resonances may be described as the exchange of n virtual bosons of energy $2\hbar kv$ similar to the high-intensity Doppleron case. In contrast to the resonance at $2kv = 2\omega_Z$ discussed above, these higher-order resonances occur at $2nkv = \omega_Z$.

Of course, increasing γ_P by increasing s or decreasing δ broadens the ground states so the resonances are washed out and the "normal" cooling to zero velocity takes over. There is clearly an optimum condition to observe the velocity-induced resonances in laser cooling where there is a balance between γ_P and ω_Z . For γ_P too small optical pumping is too weak and the atoms are not cooled; for γ_P too large the optical pumping process destroys the Zeeman coherence and therefore the resonances.

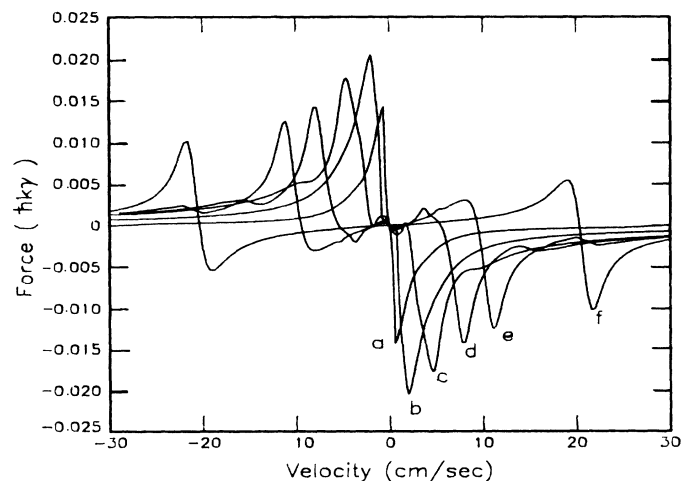


FIG. 4. The force averaged over a wavelength vs velocity for the $F=3 \rightarrow 4$ transition in ^{85}Rb for the conditions (a)-(f) as given in Fig. 2. Note the weakening of the damping near $v=0$ as the B field increases, and finally its sign reversal. Also, the resonances at v_r appear as soon as ω_Z becomes larger than γ_P .

To further compare our model with the experimental data we have numerically integrated the Fokker-Planck equation to obtain the velocity distribution after a finite interaction time. Since this time depends on the longitudinal velocity of the atoms, we have averaged this distribution over the Maxwell-Boltzmann velocity distribution of the beam. For the force in the Fokker-Planck equation, we used the calculations plotted in Fig. 4.

The diffusion contains two parts. The contribution from the fluctuation of the absorption and emission process gives a term $D_0 = \frac{7}{5} \hbar^2 k^2 \gamma_S (\sum_i C_i \rho_{ii}) / L$, where we have taken into account the multilevel structure of the atom, and the fact that levels have different transition strengths C_i . The term D_1 corresponding to the fluctuations of the magnetically induced force is calculated using the quantum regression methods outlined by Mollow.²⁰ For the $F_g = 3$ ground state in ^{85}Rb this requires solving $(2F_g + 1)^3 \sim 350$ coupled differential equations. Details on this procedure will be given in a forthcoming publication. For now we have applied this method for atoms at rest and assume that the diffusion constant is the same for moving atoms. However, at higher magnetic field the force on stationary atoms is quite different from the force on moving atoms, and this approximation may fail.

We projected the velocity distribution calculated this way into a spatial distribution in the detector plane, and plotted the results in Fig. 2 for comparison with our data. The agreement is quite good except at high magnetic field and high velocity where the approximation above for the diffusion begins to fail. To the best of our knowledge, Fig. 2 represents the first detailed comparison between experiments and the widely studied 1D models^{2,4-6} of sub-Doppler laser cooling. We think the comparison is excellent.

Cooling to nonzero velocity can have a number of important applications. First, this process can be used as an incoherent atomic beam splitter with angular separation orders of magnitude larger than from atomic diffraction by a grating.²¹ Furthermore, the angle can be swept by changing the magnetic field. Recombination of the split beam could enable collision experiments of enormous sensitivity. Second, using a standing wave along the atomic beam allows longitudinal cooling of the atoms to a finite velocity. Third, MILC can be used to eject atoms from a three-dimensional molasses to form a very well defined atomic fountain²² or slow atomic beam

with a very small velocity spread. Such monochromatic atomic beams could be used to probe the onset of slightly endothermic reactions by scanning the velocity of collision partners or surface incidence with the magnetic field.

In summary, we have discussed the importance of velocity-selective resonances for MILC. The observed splitting of the atomic beam in transverse laser cooling can stimulate new experiments in the field of high-precision atomic physics.

We acknowledge many valuable discussions with Tom Bergeman. This work was supported by the NSF and the ONR.

-
- ¹P. Lett *et al.*, Phys. Rev. Lett. **61**, 169 (1988).
²J. Dalibard *et al.*, in *Proceedings of the Eleventh International Conference on Atomic Physics, Paris, France, 1988*, edited by S. Haroche *et al.* (World Scientific, Singapore, 1989), p. 199.
³Y. Shevy *et al.*, Phys. Rev. Lett. **62**, 1118 (1989).
⁴B. Sheehy *et al.*, Phys. Rev. Lett. **64**, 858 (1990).
⁵J. Dalibard and C. Cohen-Tannoudji, J. Opt. Soc. Am. B **6**, 2023 (1989).
⁶P. Ungar *et al.*, J. Opt. Soc. Am. B **6**, 2058 (1989).
⁷A. Kazantsev, Zh. Eksp. Teor. Fiz. **66**, 1599 (1974) [Sov. Phys. JETP **39**, 784 (1974)].
⁸E. Kyrola and S. Stenholm, Opt. Commun. **22**, 123 (1977).
⁹V. Minogin and O. Serimaa, Opt. Commun. **30**, 373 (1979).
¹⁰J. Dalibard and C. Cohen-Tannoudji, J. Opt. Soc. Am. B **2**, 1707 (1985).
¹¹A. Aspect *et al.*, Phys. Rev. Lett. **57**, 1688 (1986).
¹²M. Prentiss and A. Cable, Phys. Rev. Lett. **62**, 1354 (1989).
¹³N. Bigelow and M. Prentiss (private communication).
¹⁴W. Bell and A. Bloom, Phys. Rev. Lett. **6**, 280 (1961).
¹⁵We incorrectly named half this quantity the Larmor frequency in Ref. 4.
¹⁶C. Cohen-Tannoudji, in *Frontiers in Laser Spectroscopy*, edited by R. Balian *et al.* (North-Holland, Amsterdam, 1977).
¹⁷This appeared as $\gamma'_p = 3\gamma_p$ in Ref. 4, but that is an error.
¹⁸The effective Hamiltonian H in the present basis is $H_{11} = \hbar(\tilde{\omega} - \omega_r)/2$, $H_{22} = \hbar(\tilde{\omega} + \omega_r)/2$, and $H_{12} = H_{21} = -\hbar\tilde{\omega}_{12}/2$, where $\hbar\tilde{\omega}_j$ is the light shift of the j th state, $\tilde{\omega} = \tilde{\omega}_1 + \tilde{\omega}_2$ and $\tilde{\omega}_{12} = \tilde{\omega}_1 - \tilde{\omega}_2$.
¹⁹S.-Q. Shang and H. Metcalf, Appl. Opt. **28**, 1618 (1989).
²⁰B. R. Mollow, Phys. Rev. **188**, 1969 (1969).
²¹D. W. Keith *et al.*, Phys. Rev. Lett. **61**, 1580 (1988).
²²M. Kasevich *et al.*, Phys. Rev. Lett. **63**, 612 (1989).